Bollettino di Geofisica Teorica ed Applicata Vol. 55, n. 3, pp. 683-697; September 2014
DOI 10.4430/bgta0128

# Detecting and modelling the evaporate dome in a dam site using microgravity data

V.E. Ardestani

*Institute of Geophysics, University of Tehran, and Centre of Excellence in Survey Engineering and Disaster Management, Tehran, Iran*

(Received: February 24, 2013; accepted: April 7, 2014)

***ABSTRACT*** A microgravity survey was carried out at a dam site with a hilly topography inside the microgravity network and a rough terrain in the surrounding area for mapping the evaporate dome. After applying Earth tide, free-air and Bouguer corrections, the Bouguer gravity anomalies were computed. Using the polynomial fitting approach, the residual gravity anomalies were obtained. Several relative negative anomalies were distinguishable in the residual map. Rough estimations of the minimum and maximum depths of these anomalies were provided by Euler de-convolution and upward continuation methods. These anomalies were modelled by the three-dimensional (3D) inversion method.

**Key words:** microgravity data, evaporate dome, detecting, 3D modelling.

## 1. Introduction

Detection of the evaporate domes is one of the most frequently cited applications of the gravity method. The most defined and known evaporates investigated by gravity data include salt and gypsum.

Nettelton (1976) reported one of the first applications of the method in salt dome (Humble salt dome) detection. Gravity data on the Humble salt dome has been used by several researchers, such as Abdolrahman *et al*. (1989, 1999) and Aghajani *et al*. (2009), to estimate the shape and depth of the salt dome.

In general, the evaporate dome can be constructed from salt, gypsum, etc. and has been investigated in several engineering projects by microgravity data such as those by Butler and Yule (1984) and Al-Rawi *et al*. (1989). These evaporates are mostly accompanied by solution cavities such as sink-holes and cavities. Colley (1962) reported the first work in the detection of cavities in Iraq by using gravity measurements. Ardestani (2013) reported the detection and modelling of solution cavities in evaporate dome in a dam site.

The microgravity survey, which offers direct information about density distribution, is one of the most powerful methods for detecting subsurface evaporates. Although the method is simple in principle, it requires a strict data acquisition procedure and quality control, careful data correction and sophisticated data analysis and interpretation.

Qualitative and quantitative interpretation methods (after gravity corrections) can be used to identify unknown parameters such as density contrast and the geometry of the causative source.

 

Gravity modelling by inversion of gravity data plays a vital role in quantitative interpretation. There are several methods to invert gravity or microgravity data. One of these methods, based upon the exploration of model possibilities, is identified by Camacho *et al*. (2011). In this paper, we focus upon detecting the evaporate dome in the west bank of the reservoir of the Rogun dam site in Tajikistan.

## 2. Location and geology of the survey area and project target

The area under consideration is located in a region with a rough topography close to the city of Rogun in Tajikistan where a dam is constructed (Fig. 1). There is a hilly topography in the survey area with very steep slopes in the east and south where it encounters the river valley.

The main geological units in the survey area are as follows (OSHPC Barki Tojik, 2012):

- Cretaceous: silt, mud, sandstone, granodiorite, conglomerate and limestone;
- Triassic: evaporates (gypsum and halite).

The geological map is shown in Fig. 2, where the prospected area for the microgravity survey is marked.

The interpretation process is quite complex due to the closeness of the densities of the constructing materials and very rough topography of the surrounding area. There are several solution cavities in the salt member of the evaporate formation which are outcropped with the sinkholes in the area. The solution cavities in evaporate dome around the reserve of the dam

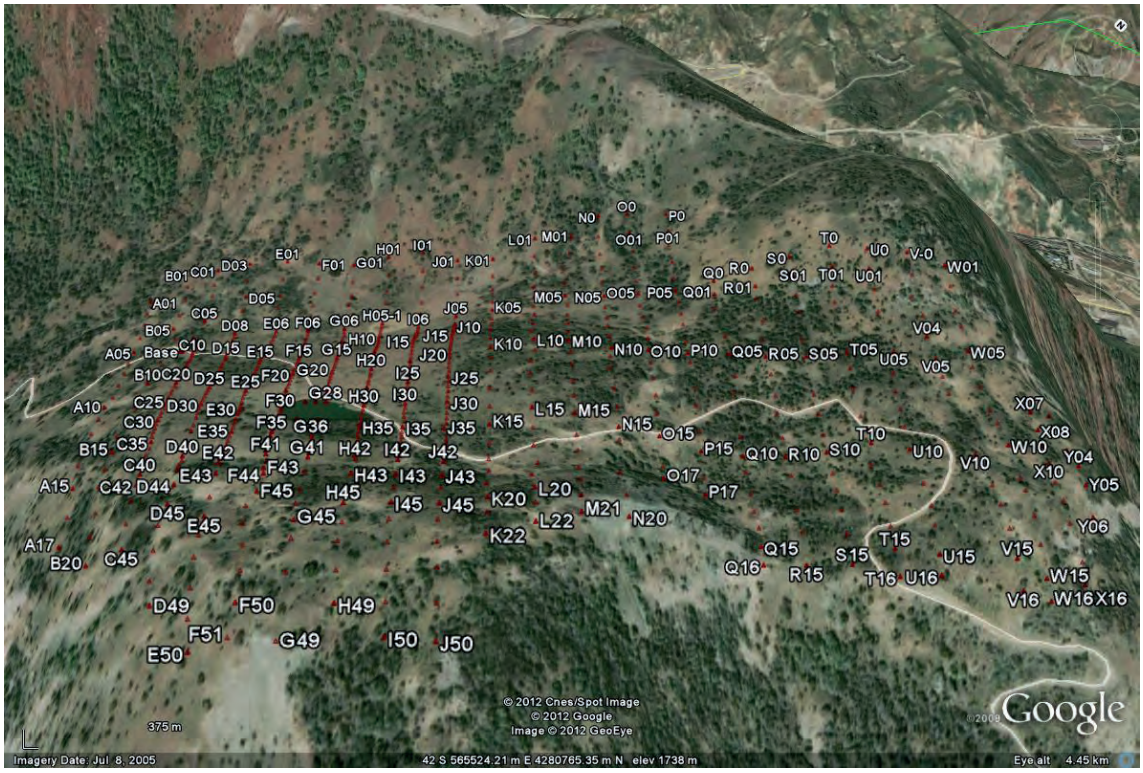


Fig. 1 - Site area including microgravity network in Google Earth.

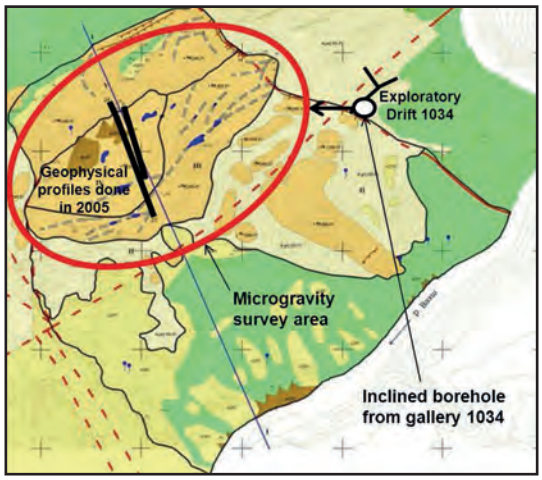


Fig. 2 - Geology of the survey area.

site can cause leakages of the water. On the other hand, they may cause sever damage to the foundations of dams.

The microgravity survey area is defined based upon some (existing?) geological assumptions of the probable (existing?) evaporate dome after encountering a borehole to the thick layer of gypsum with thin marlstone and clay stone interbedded. These evaporates may be deeply-rooted and affect the overlain layers as a dome. As the area including the dome is located in the reservoir of the dam, the depth and eastern extension towards the river of this probable dome is of some importance for the engineers.

## 3. Field procedures

Data were collected using a Scintrex CG3 gravimeter with a sensitivity of 5 μGal at about 700 stations at 10 to 30 m intervals along the profiles and 50 m distance between the profiles. Station altitude was measured by a Trimble Dual Frequency GPS with about 1 cm accuracy in the horizontal and vertical coordinates (x, y, h). The gravity measurements were undertaken by the gravity branch of the Institute of Geophysics, Tehran University, in October 2012 and under the supervision of the author (the author was the director, executor and interpreter of the project).

## 4. Gravity corrections

The raw gravity measurements were tied to a base point in the lowest part of the topography. The long-term drift of the gravimeter was removed by using the cycling mode of the gravimeter over several days at the office in Tehran. For removing the short-term drift, the gravity was measured on the base point every two hours. The maximum short-term drift during a day was 30 μGal.

The tidal correction was also computed and data was recorded by the gravimeter. This means that the downloaded raw data is the sum of the reading value and the tidal effects.

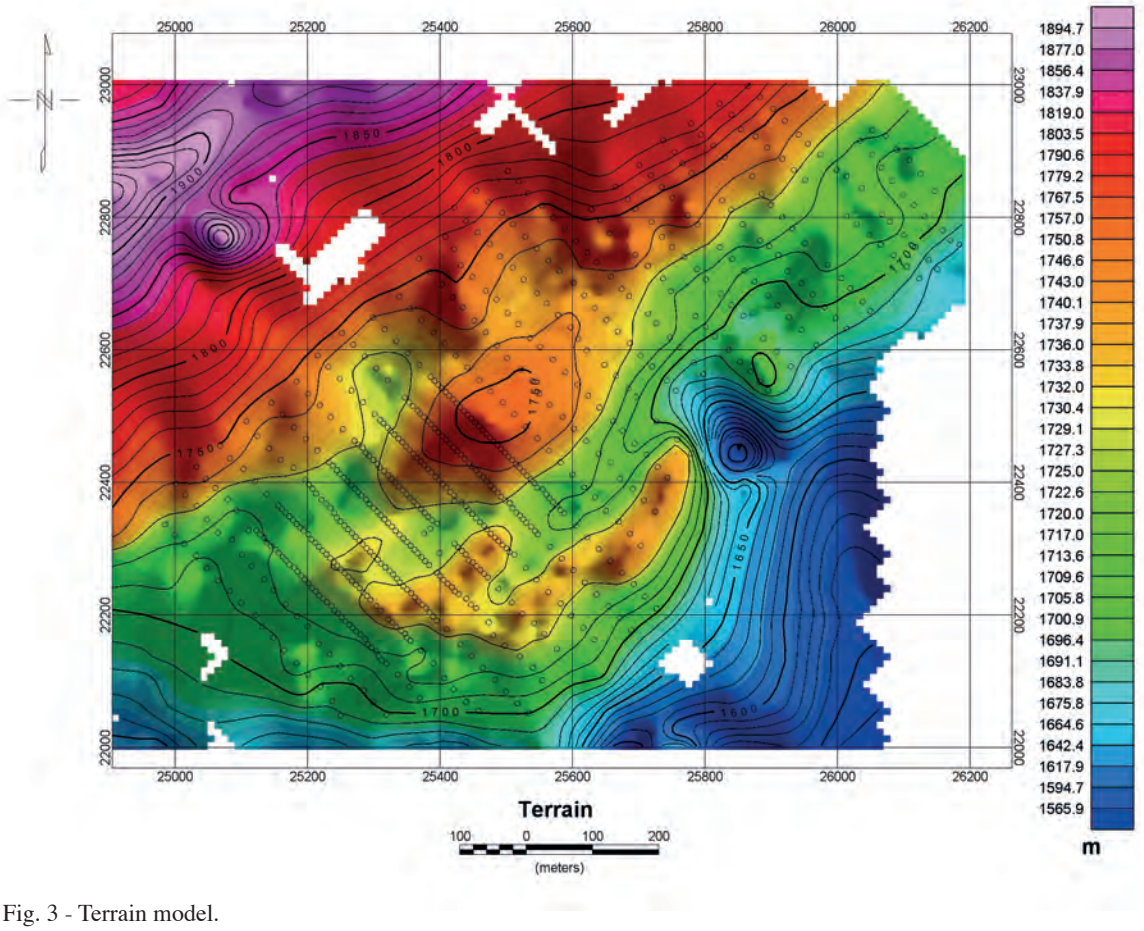


Fig. 3 - Terrain model.

The data were, then, corrected for effects caused by variations in latitude, elevation and topography using standard formulas (Telford *et al*., 1981). The terrain correction was the most sensitive stage in reductions due to the rough topography of the site area. These corrections are calculated using a combination of the methods described by Nagy (1966) and Kane (1962). In order to calculate local corrections, the local digital terrain model (DTM) is "sampled" to grid mesh centred on the station to be calculated. The terrain map of the area and surrounding area is reflected in Fig. 3.

The correction is calculated based on near zone, intermediate zone and far zone contributions. In the near zone (0 to 1 cells from the station), the algorithm sums up the effects of four sloping triangular sections, which describe a surface between the gravity station and elevation at each diagonal corner (Kane, 1962). In the intermediate zone (1 to 8 cells from the station), the terrain effect is calculated for each point using the flat topped square prism approach of Nagy (1966). In the far zone (greater than 8 cells) the terrain effect is derived from the annular ring segment approximation to a square prism as described by Kane (1962). As the height of gravity points are measured accurately, we included these points in the DTM to make it as dense as possible. The topographical corrections are demonstrated in Fig. 4. After the corrections, the Bouguer gravity anomalies were computed and are shown in Fig. 5. The statistical values of topographical corrections and Bouguer anomalies are reported in Table 1.

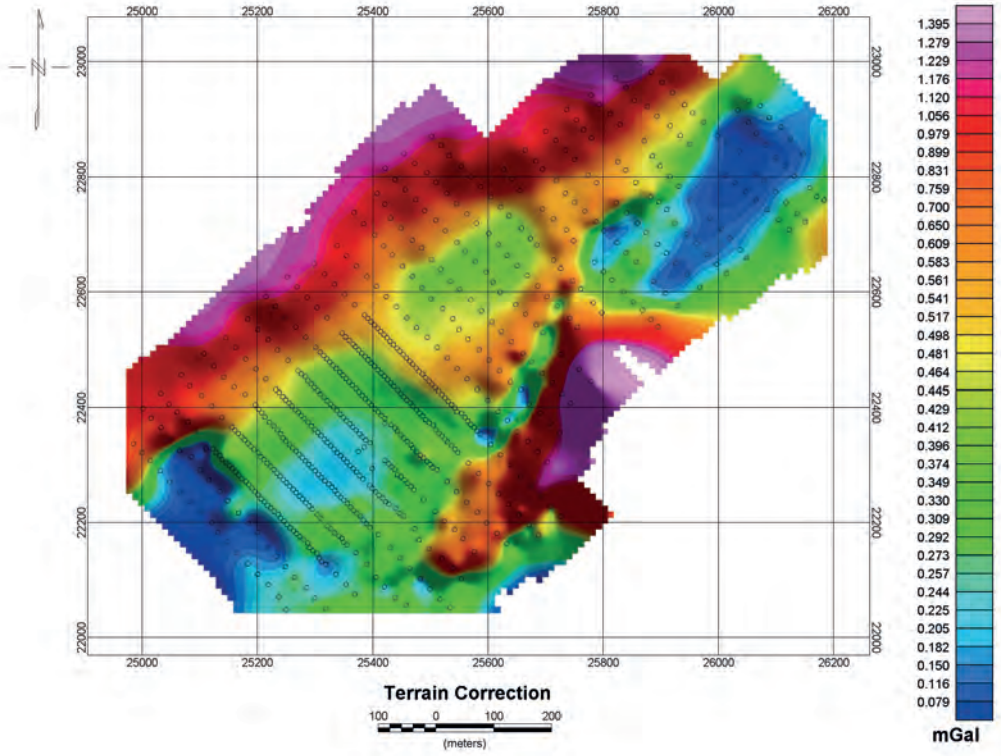


Fig. 4 - Terrain corrections (mGal).

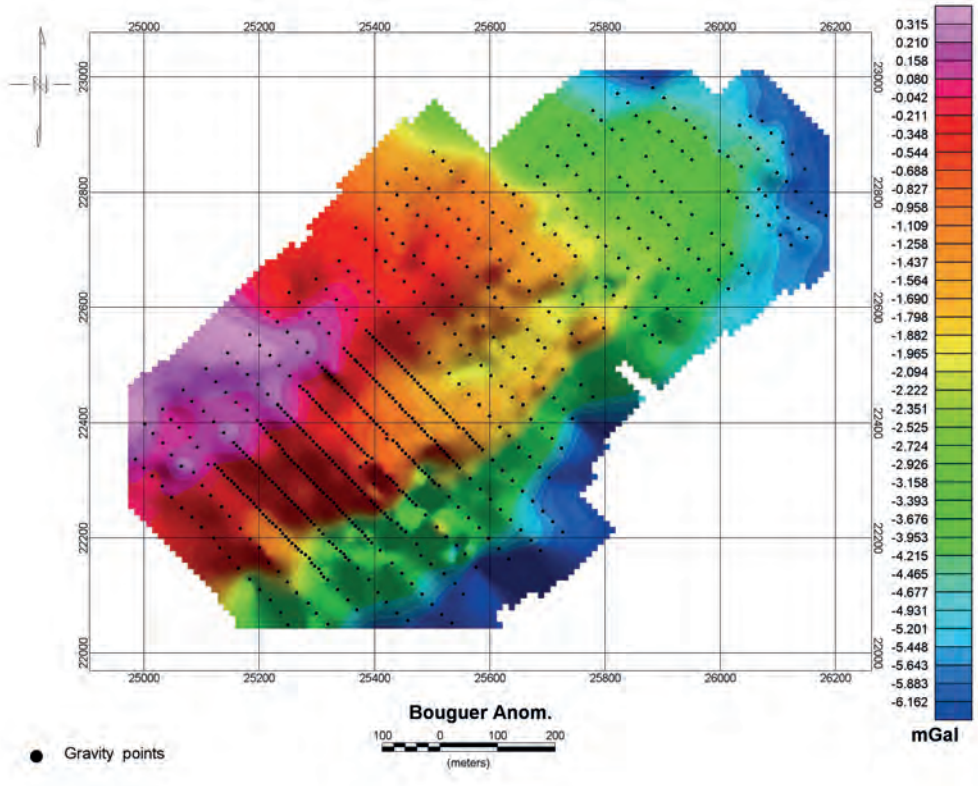


Fig. 5 - Bouguer anomalies (mGal).

Table 1 - Statistical values of topographical corrections and Bouguer anomalies.

| Values | Minimum (mGal) | Maximum (mGal) | Average (mGal) | Standard Deviation (mGal) |
|---|---|---|---|---|
| Topographical Corrections | 0.017 | 2.49 | 0.576 | 0.391 |
| Bouguer anomalies | -7.1 | 0.3 | -2.48 | 1.93 |

The values of topographical corrections seem to be quite reasonable in comparison with the Bouguer anomalies values in Table 1. However, an inspection of Fig. 4 shows that the digital terrain model has no proper coverage in east and west directions where there is very rough topography. In any case, due to the shortage of time and the limited budget, we performed the terrain correction using the terrain model reflected in Fig. 3.

## 5. Interpretation process

The interpretation process is based upon detecting negative anomalies. The respective negative local anomalies may be caused by evaporates and their solution cavities.

The interpretation starting point is the map of Bouguer anomalies (Fig. 5). An inspection of this figure shows that the regional anomalies are quite dominant. The regional trend was separated by second order polynomial fitting to make the residual anomalies that are shown in Fig 6, where several relative negative anomalies are detected, some of which are located in the border of the microgravity network. The negative anomaly zones indicate a mass depletion region which may be associated with evaporate dome affected by solution cavities.

The most conspicuous feature is broad negative anomaly number 1 in Fig. 6 and close to the drilled borehole (DZ2).

For primary estimation of the minimum depths of these anomalies, the Euler de-convolution method is used and the results are demonstrated in Fig. 7. This figure shows the Euler depths projected in the residual anomalies of Fig. 6. The Euler depths are computed by the following equation (Thompson, 1982):

$$\left(x-x_0\right)\frac{\partial g}{\partial x}+\left(y-y_0\right)\frac{\partial g}{\partial y}+\left(z-z_0\right)\frac{\partial g}{\partial z}=Ng \qquad (2)$$

where $x_0$, $y_0$, $z_0$ are the coordinates of a point of the underground anomaly and $N$ is the structural index. The maximum depths of the anomalies are computed by upward continuation and the results are shown in Figs. 8 and 9. The upward continuation is computed by way of Fourier transform (Blakely, 1997). According to the principle identified by Jacobson (1987), the distance of upward continuation can be considered as the distance of downward continuation. The maximum depth of the anomaly is actually the distance at which the effect of the anomaly has disappeared. This makes a rough estimation for the maximum depth of the gravity anomalies which is the most difficult unknown parameter for estimation purposes. These depths will be compared to the depths estimated through the modelling process in the next section.

In order to obtain a rough estimation of the density contrast, the apparent densities are computed (Oasis Montaj, Version 8) and shown in Fig. 10.

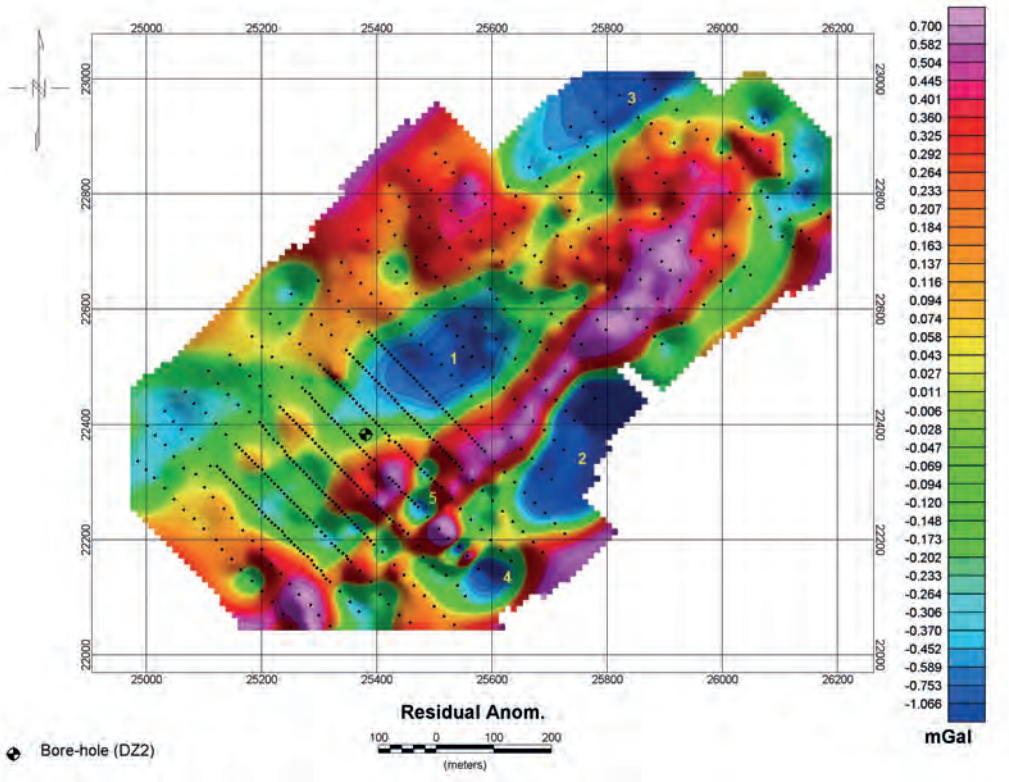


Fig. 6 - The residual anomalies by removing the trend surface of degree 2 (mGal).

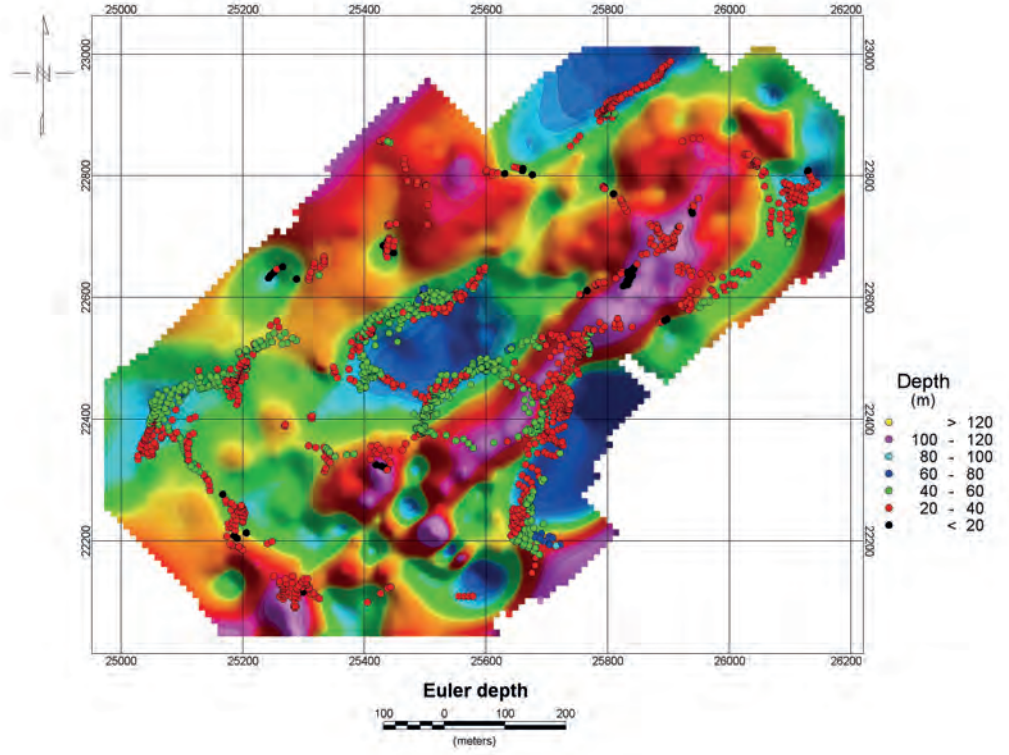


Fig. 7 - Euler depths of residual anomalies in (m).

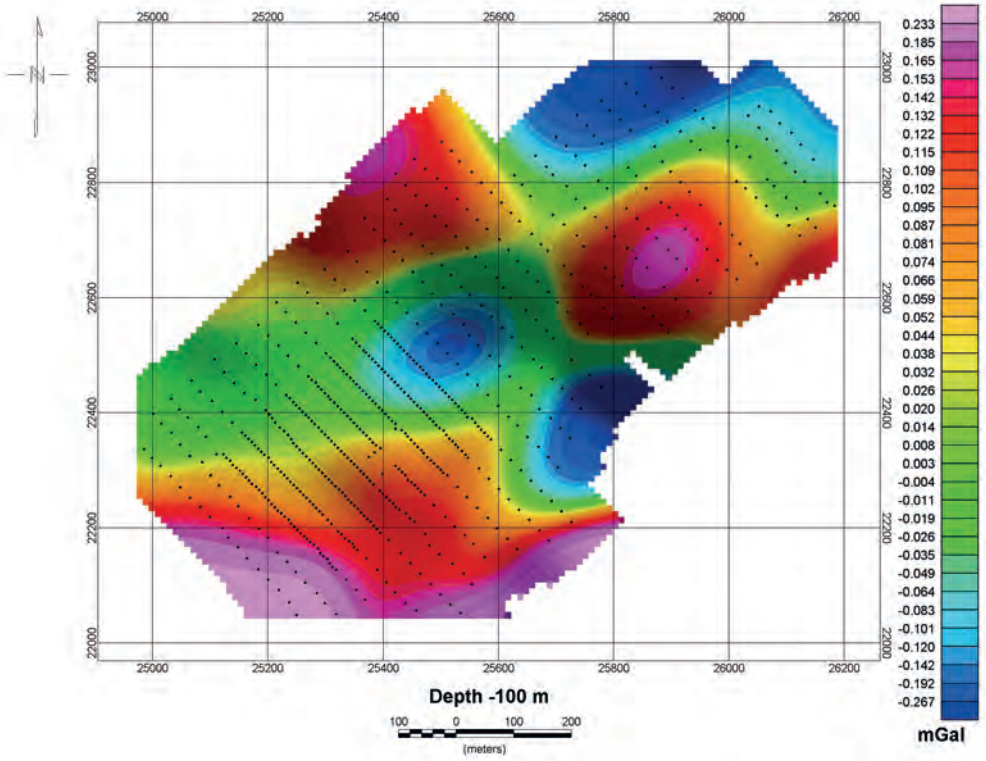


Fig. 8 - Residual anomalies in depth of about 100 m (mGal).

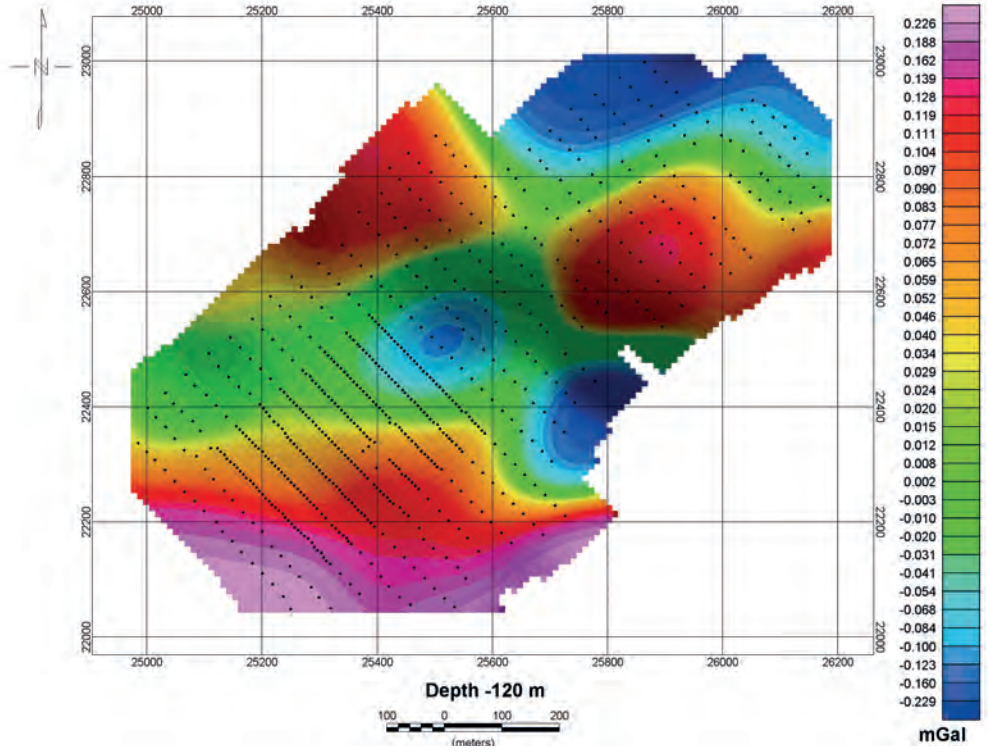


Fig. 9 - Residual anomalies in depth of about 120 m (mGal).

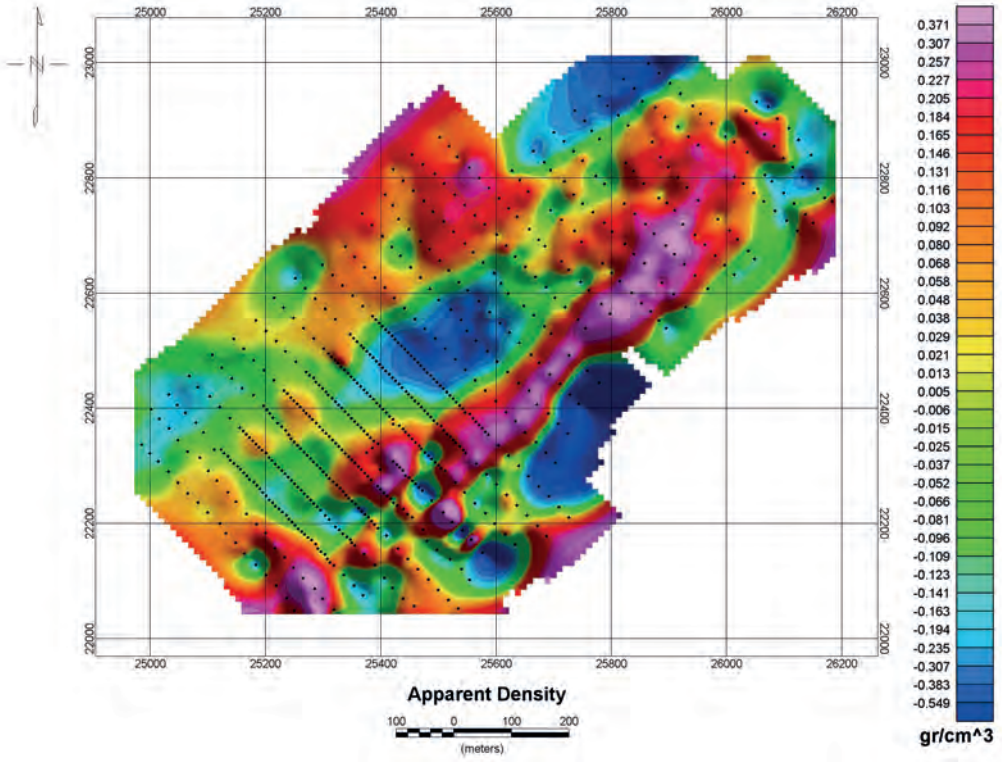


Fig. 10 - The apparent densities (kg/m$^3$).

## 6. 3D modelling

The 3D inversion method described by Camacho *et al*. (2011) was applied in order to model the main low density zone (number 1 in Fig. 6) in the window shown in Fig. 11. They represent an inversion package (GROWTH2.0) which is quite straightforward and user-friendly.

The results of 3D modelling for the selected window are reflected in Figs. 12 to 16. These figures show the X and Y slices and the horizontal sections of density contrasts from 1750 m to 1630 m heights.

By inspecting the figures, the density contrasts and the depths of the anomalies can be readily estimated. It is worth noting that the geological map is used as prior information in the modelling process. For example, when defining the upper and lower bands of density contrast and the borehole, it is used to validate the results.

The results of the interpretation process and 3D modelling are summarised in Table 2.

Table 2 - Results of the interpretation process and 3D modelling.

| No. of anomaly | Maximum height of the ground surface (m) | Minimum depth through modelling (m) | Maximum depth through Modelling (m) | Maximum Density Contrast through modelling (gr/cm$^3$) | Maximum Density Contrast through Apparent density (gr/cm$^3$) | Minimum depth through Euler (m) | Maximum depth through depth maps (m) |
|---|---|---|---|---|---|---|---|
| 1 | 1754 | - | 120-130 | -0.4 | -0.4 | 20 | 120 |

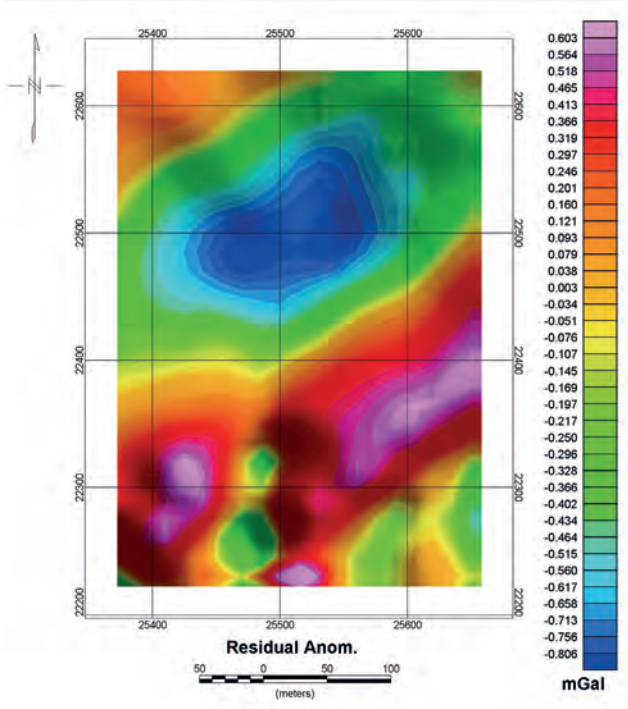


Fig. 11 - The window of residual anomalies for 3D modelling (mGal).

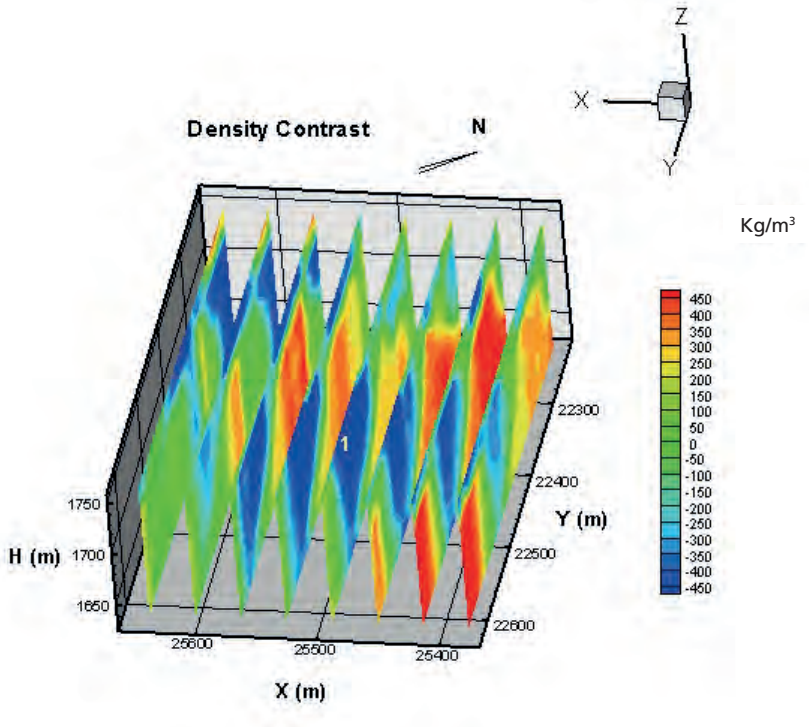


Fig. 12 - X slices of density contrasts (kg/m$^3$).

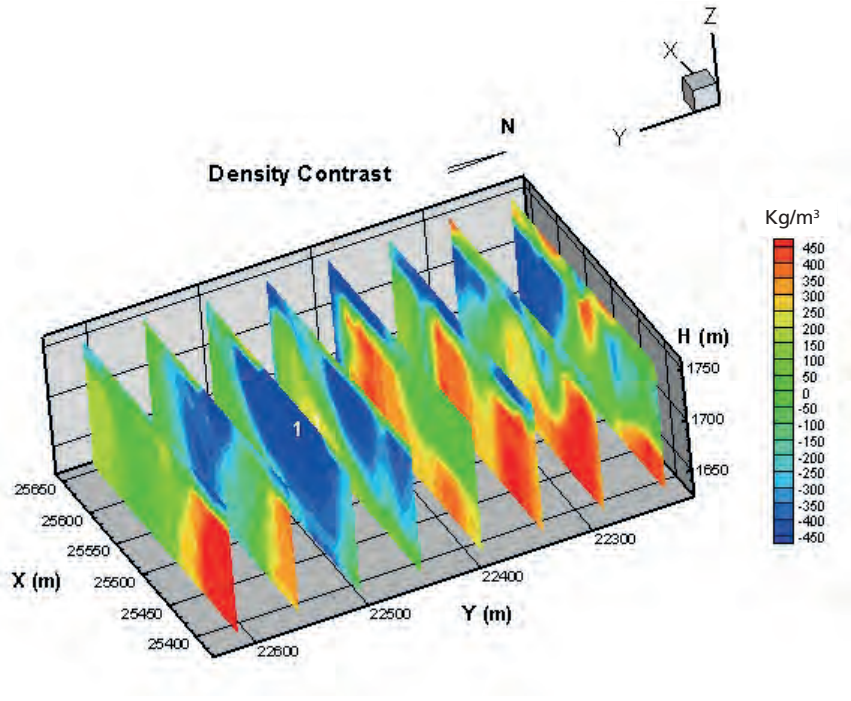


Fig. 13 - Y slices of density contrasts (kg/m$^3$).

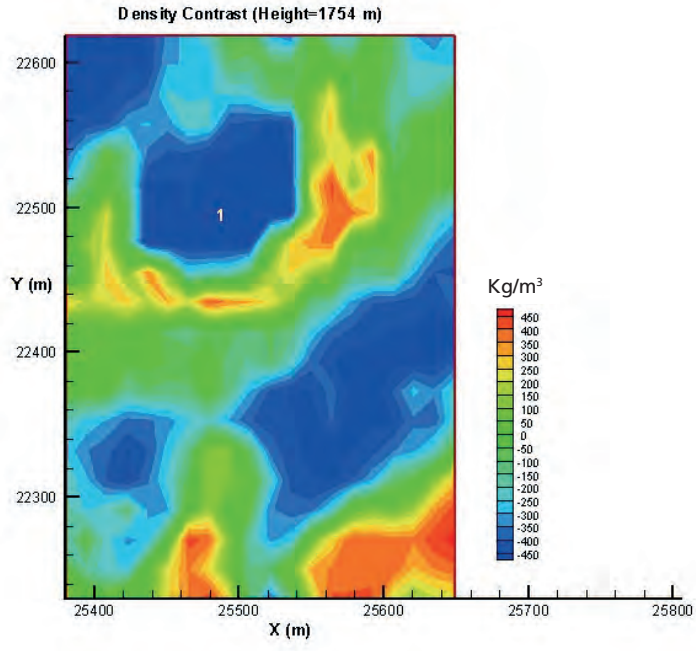


Fig. 14 - Horizontal slice of density contrasts in 1754 m height (kg/m$^3$).

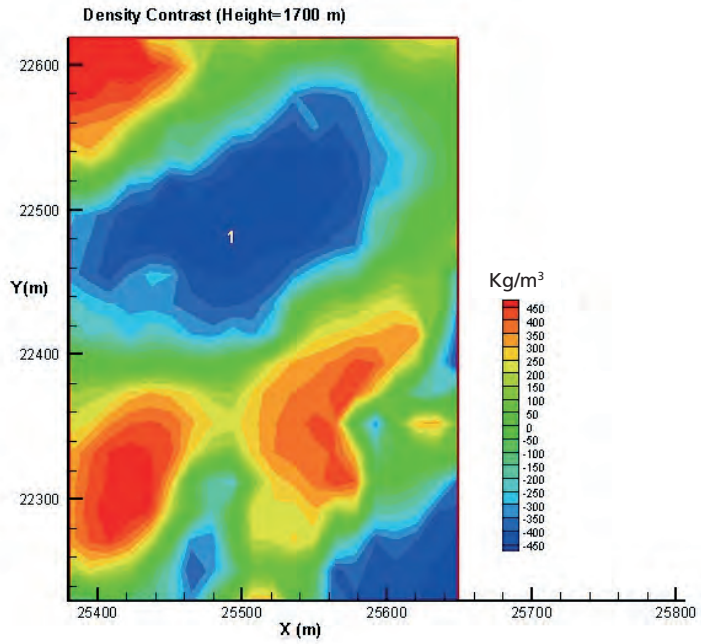


Fig. 15 - Horizontal slice of density contrast in 1700 m height (kg/m$^3$).

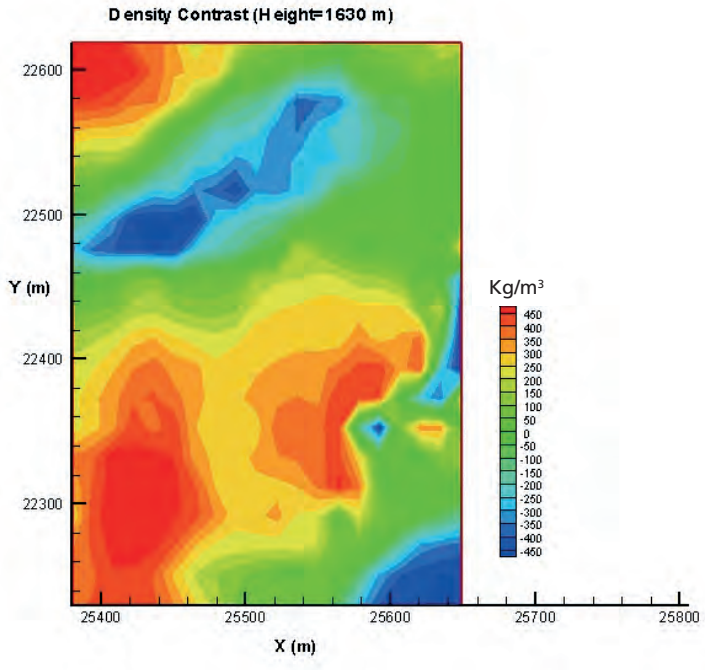


Fig. 16 - Horizontal slice of density contrast in 1630 m height (kg/m$^3$).

## 7. The borehole

One borehole is drilled before the microgravity survey is carried out. This borehole (Fig. 6) encounters the evaporate deposit such as gypsum. The depths of the encountered deposits in the borehole are reflected in Table 3.

Table 3 - Borehole DZ2.

| Geological units | Depth (m) | |
|---|---|---|
| - | To | From |
| Overburden, Clay with Silt | 68 | 0 |
| Shaly Limestone | 74 | 68 |
| Gypsum and Clay stone sequence | 166 | 74 |

## 8. Discussion

The results for depth estimation of anomaly number 1 show that this anomaly begins from shallow depths (nearly ground surface in modelling and 20 m in Euler) and continues to about 120 m depth. By inspecting Table 3, we conclude that various geological units may be involved in generating this anomaly. In fact, we can expect a large low-density zone from near the ground surface to the depth of about 120 m via the results of modelling and several other filters (Table 2). This low-density zone does not expand to the eastern area, which is very critical for construction of the dam based on the 3D modelling results (Figs.12 to 16).

One of the very useful items of information that can be obtained through the inversion package (GROWTH2.0) is the centre of the mass. The output of the package is presented in Fig. 17. Considering the coordinates of the centre of the negative mass in Fig. 17, the z coordinate is 1680 m which, if subtracted from the height of the ground surface at this point (1752 m), obtains 72 m. This depth (72 m) is very close to the border of the overburden and shaly limestone (68 m) observed in borehole DZ02 (Table 3). This may show the importance of this contact surface.

The next issue to address is the cause of this low-density zone (anomaly number 1). The first possibility may be the existence of salt masses and gypsum which are deeply rooted and affect the overlain layers as a dome.

The second possibility is the cavities and sink areas with clay fill in the overburden, particularly in the interface of over burden and the shaly limestone and in the gypsum sequence. The salt masses or gypsum that cause this anomaly may have small cavities based upon my own experience in the sites similar to the survey area with similar geological units (clay, silt, gypsum and salt) and considering the maximum density contrast (about -0.4 gr/cm$^3$) and the closeness of the densities of clay, silt, gypsum and salt.

## 9. Conclusion

The evaporate dome can be detected by way of microgravity data in relatively rough

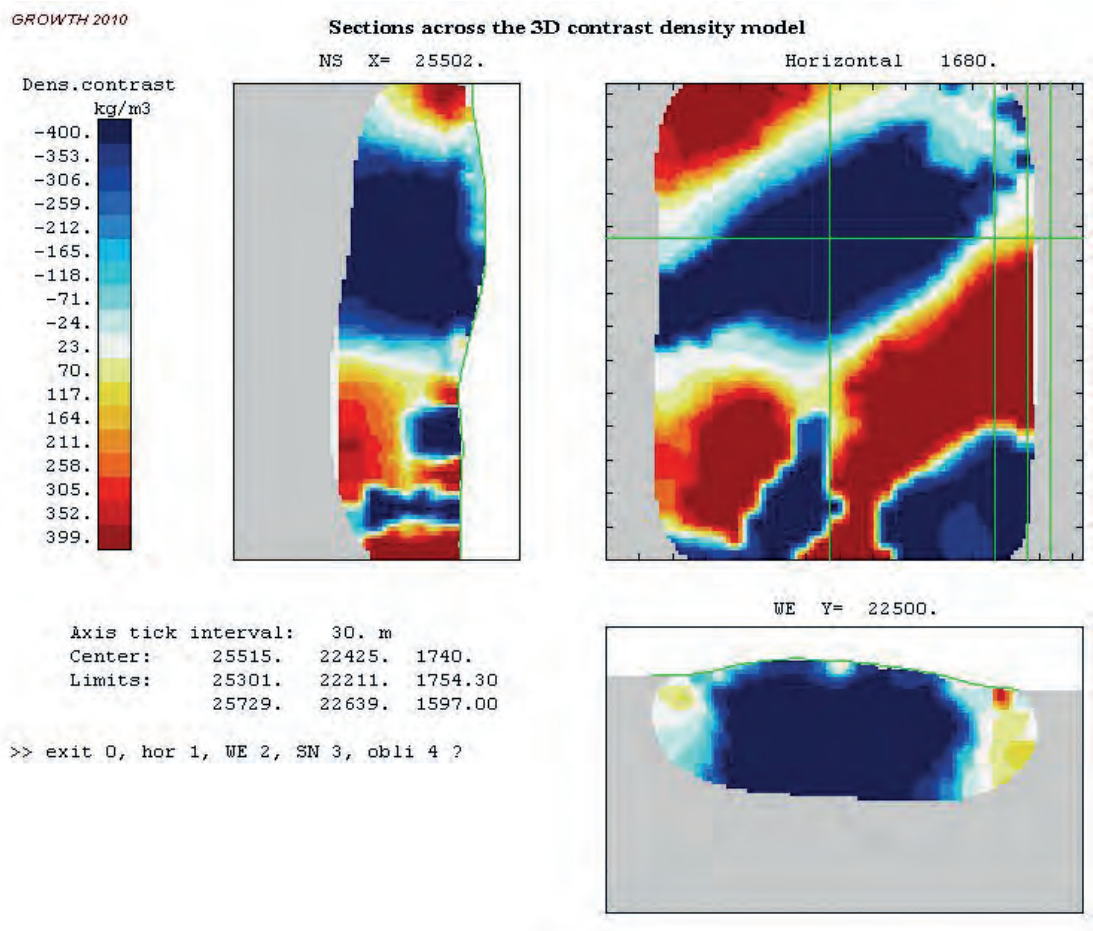


Fig. 17 - Cross sections of density contrasts in centre of negative mass, x=25502 m and y=22500 m and z=1680 m .

topography. This method can even be used when a low density contrast exists and the geological structures are very complex until the signal definitely exceeds the noise-range (about 20 μGal after corrections and processing). The folding of evaporate dome is the precondition of its detection by the microgravity method.

However, some existing information through a small number of boreholes is extremely vital to the accuracy of the interpretation results and the results can be checked and revised based upon the information. The depths obtained from one borehole close to the main negative anomaly confirm the minimum depths computed by the Euler method and 3D modelling. The observed maximum depths of evaporates in the borehole shows that the maximum depths estimated through upward continuation and 3D modelling are relatively accurate just in the centre area of the microgravity network.

**Acknowledgments.** Special thanks should be given to Pars Tunnel Consulting Engineering Company authorities, particularly the engineers Binazadeh, Farazmand and Chehreh for all their support. The author is grateful to the authorities of the Institute of Geophysics, the University of Tehran for the support provided and to Mr Salimi for measuring the data. Special thanks should also be given to the Government of Tajikistan and to authorities in any way involved in the dam project for their hospitality.

REFERENCES

Abdolrahman E.M., Boyoumi A.L., Abdelhady Y.E., Gobashy M.M. and El-Araby H.M.; 1989: *Gravity interpretation using correlation factors between successive least-squares residual anomalies*. Geophysics, **54**, 1614-1621.

Abdolrahman E.M., Abo-Ezz E.R, Anwer H. and Radwan H.A.; 1999: *A numerical approach to depth determination from residual gravity anomaly due to two structures*. Pure and Applied Geophysics, **154**, 329-341.

Aghajani H., Moradzadeh A. and Hualin Z.; 2009: *Estimation of depth to salt domes from normalized full gradient of gravity anomaly and examples from the USA and Denmark*. Journal of Earth Science, **20**, 1012-1016.

Al-Rawi F.R., Al-Badri A.S. and Rezkalla J.S.; 1989: *Application of microgravimetric in Samava salt deposit, Iraq*. Geophysics, **54**, 440-444.

Ardestani V.E.; 2013: *Detecting, delineating and modeling the connected solution cavities in a dam site via microgravity data*. Acta Geodaetica and Geophysica, **48**, 123-138.

Blakely J.R.; 1997: *Potential theory in gravity and magnetic applications*. Cambridge University Press, 441 pp.

Butler D.K. and Yule D.E.; 1984: *Microgravity survey of Wilson dam powerplant switchyards, Florence, Alabama*. Misc. Paper GL-84-16, U.S. Army Engineers Waterways Experiment Station Vicksburg, Tennessee Valley Authority, 29 pp.

Camacho A.G., Fernandez J. and Gottsmann, J.; 2011: *3-D gravity inversion package GROWTH2.0 and its application to Tenerife Island, Spain*. Computers & Geosciences, **37**, 621-633.

Colley G.C.; 1962: *The detection of caves by gravity measurements*. Geophysical Prospecting, **11**, 1-9.

Jacobson H.; 1987: *A case for upward continuation as a standard separation filter for potential field maps*. Geophysics, **52**, 1138-1145.

Kane M.F.; 1962: *A comprehensive system of terrain corrections using a digital computer.* Geophysics, **27**, 455-462.

Nagy D.; 1966: *The gravitational attraction of a right rectangular prism*. Geophysics, **31**, 362-371.

Nettelton L.L.; 1976: *Gravity and magnetic in oil prospecting*. McGraw-Hill Book Com., 480 pp.

OSHPC Barki Tojik; 2012: *Techno-economic assessment study for Rogun hydroelectric construction project*. Report No. P.002378 RP 6, 16 pp.

Thompson D.T.; 1982: EULDPH: *a new technique for making computer-assisted depth estimates from magnetic data*. Geophysics, **47**, 31-37.

Telford W.M., Geldart L.P., Sheriff R.E. and Keys D.A.; 1981: *Applied geophysics*. Cambridge University Press, Cambridge, New York, U.S.A., 792 pp.

Corresponding author: Vahid E. Ardestani
Institute of Geophysics, University of Tehran, and Centre of Excellence in Survey Engineering and Disaster Management
Kargar Shomali, Tehran, Iran
Phone: ; fax: ; e-mail: ebrahimz@ut.ac.ir